Searches for light sterile neutrinos with multitrack displaced vertices

Giovanna Cottin[*]

Cavendish Laboratory, University of Cambridge, Cambridge CB3 0HE, United Kingdom
and Department of Physics, National Taiwan University, Taipei 10617, Taiwan

Juan Carlos Helo[†]

Departamento de Física, Facultad de Ciencias, Universidad de La Serena,
Avenida Cisternas 1200, La Serena, Chile
and Centro-Científico-Tecnológico de Valparaíso, Casilla 110-V, Valparaíso, Chile

Martin Hirsch[‡]

AHEP Group, Instituto de Física Corpuscular - C.S.I.C./Universitat de València,
Edificio de Institutos de Paterna, Apartado 22085, E–46071 València, Spain

We study discovery prospects for long-lived sterile neutrinos at the LHC with multitrack displaced vertices, with masses below the electroweak scale. We reinterpret current displaced vertex searches making use of publicly available, parametrized selection efficiencies for modeling the detector response to displaced vertices. We focus on the production of right-handed W_R bosons and neutrinos N in a left-right symmetric model, and find poor sensitivity. After proposing a different trigger strategy (considering the prompt lepton accompanying the neutrino displaced vertex) and optimized cuts in the invariant mass and track multiplicity of the vertex, we find that the LHC with $\sqrt{s} = 13$ TeV and 300 fb^{-1} is able to probe sterile neutrino masses between 10 GeV $< m_N <$ 20 GeV (for a right-handed gauge boson mass of 2 TeV $< m_{W_R} <$ 3.5 TeV). To probe higher masses up to $m_N \sim 30$ GeV and $m_{W_R} < 5$ TeV, 3000 fb^{-1} will be needed. This work joins other efforts in motivating dedicated experimental searches to target this low sterile neutrino mass region.

I. INTRODUCTION

With the discovery of the Higgs boson [1,2], the Large Hadron Collider (LHC) has confirmed the particle content of the Standard Model (SM). Still one of the main unanswered fundamental questions is the origin of neutrino masses. Experimental data on neutrino oscillations [3] provides clear evidence that there must be new physics beyond the SM, whose effects are actively being looked for by the LHC experiments.

The smallness of neutrino masses may be explained by the so-called seesaw mechanism [4], introducing the existence of massive, right-handed (i.e. sterile) neutrinos [5,6] (see Ref. [7] for a comprehensive review). Different realizations of this mechanism give rise to sterile neutrinos with Majorana masses covering various mass ranges (for a more extensive discussion on collider searches and limits, see Refs. [8–10] and references therein). Particularly in left-right symmetric extensions of the SM [11,12], the production and decay of the sterile neutrino N depends mostly on the unknown mass of the new, heavy right-handed gauge boson, W_R.

In the mass region where $m_N \ll m_{W_R}$, the distinctive (lepton-number-violating) signature of same-sign dileptons [13] has been extensively studied [8–10,14–22]. If the sterile neutrino mass is also below the electroweak scale (i.e. $m_N < m_W$), it can be long-lived, and travel a measurable distance before decaying inside the LHC detectors.

Different collider searches for long-lived sterile neutrinos have been studied in Refs. [23–35]. At the LHC, these include signatures of trileptons [25,32], lepton jets [29,32], displaced "neutrino jets" [25,30], displaced vertices from Higgs decays [31,33] and displaced vertices, defined in a broad sense [35].

These distinct search proposals target different neutrino mass regions. For example, 13 TeV searches for "neutrino jets" can reach neutrino masses of order hundreds of

[*]gcottin@phys.ntu.edu.tw
[†]jchelo@userena.cl
[‡]mahirsch@ific.uv.es

GeV [30]. In this work we are interested in $\mathcal{O}$ (10 GeV) neutrinos. Displaced lepton-jet searches can place strong limits on sterile neutrinos in the (4–25 GeV) mass range [29]. Here we propose a complementary search for displaced vertices, that has the advantage of zero background.

This work considers a different search strategy, in which events are triggered by a prompt lepton and the neutrino charged decay products are identified to come from a common displaced vertex (DV), where a detailed detector response to displaced vertices is implemented in the form of parametrized selection efficiencies, recently made public by the ATLAS Collaboration [36].

Our search proposal is inspired by the ATLAS multi-track displaced vertex analysis [37,38]. This work particularly expands the previous work in Ref. [35] by considering a smaller fiducial region for displaced decay lengths, in order to have decays limited to the inner trackers of the LHC detectors (<300 mm) and by accurately modeling the detector response to displaced vertices inside them. In addition, our search strategy differs from the one in Ref. [35] by triggering on the prompt lepton, instead of placing cuts on leptons and/or jets coming from the displaced vertex, and, by reconstructing the displaced vertex position from the neutrino charged decay products (i.e. tracks).

The rest of the paper is structured as follows. We briefly review the phenomenology of left-right symmetric models in Sec. II. In Sec. III we discuss on our proposed DV strategy and discovery prospects at the LHC. Concluding remarks are presented in Sec. IV.

II. LEFT-RIGHT SYMMETRIC MODEL

The model considered is the left-right symmetric extension of the SM [11,12,39], with gauge group $SU(2)_L \times SU(2)_R \times U(1)_{B-L}$ and couplings g_L, g_R, g_1, respectively. This model contains a right-handed gauge boson W_R and three right-handed Majorana neutrinos, with lightest state N. In the mass range we are interested in (i.e. $m_N \ll m_{W_R}$, $m_N < m_W$), the sterile neutrino proper decay length can be written as [35,40,41]

$$c\tau_N \sim 0.12 \left(\frac{10 \text{ GeV}}{m_N}\right)^5 \left(\frac{m_{W_R}}{1000 \text{ GeV}}\right)^4 \text{ [mm]}. \quad (1)$$

A diagram showing sterile neutrino production and decay at the LHC can be seen in Fig. 1.

This process leads to different signatures, depending on the neutrino lifetime and mass. Existing searches by ATLAS [42] and CMS [43] place a lower limit on m_{W_R} at 3 TeV, for $0.2 \text{ TeV} \lesssim m_N \lesssim 2 \text{ TeV}$. CMS has recently excluded right-handed bosons with masses $m_{W_R} < 4.4 \text{ TeV}$, for $m_N = m_{W_R}/2$ [44]. Searches for new resonances in the dijet distribution can also be used to place limits on right-handed bosons [45–47], roughly of order 3 TeV. For neutrino decays
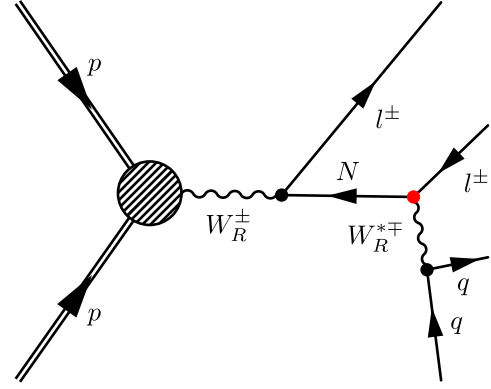

FIG. 1. Sterile neutrino N production and decay at the LHC in the left-right symmetric model. For $m_N \ll m_{W_R}$, production proceeds through a W_R, followed by N displaced decay to a lepton and quarks. The displaced vertex position is represented by the red circle.

outside of the detector, searches for new heavy gauge bosons decaying to leptons and missing transverse momentum [48,49] can be sensitive.

Early constraints on left-right symmetric models from LHC data have been addressed in Ref. [50]. The very recent study in Ref. [51] tried to systematically asses constraints covering the entire neutrino mass range, and explored sensitivity from different searches. For decays in the "displaced region" in the authors' definition, displaced jets searches (see for example Ref. [52]) can be effective.

Currently, no public searches at the LHC target sterile neutrinos with masses as low as a few GeV.

In the rest of the paper we restrict our discussion to sterile neutrino mixing with the electron sector only, for simplicity.

III. SIMULATION AND RESULTS

We generate a UFO [53] model with SARAH [54] and use SPHENO [55,56] for the spectrum calculation of the left-right symmetric model. The SARAH model files are taken from the implementation of the left-right symmetric model given in [57]. We simulate events for the process $pp \rightarrow W_R^\pm \rightarrow Ne^\pm$. Generation is performed with MADGRAPH5_AMC@NLOV2.4.3 [58] at leading order. The output corresponds to unweighted events in LHE format [59]. The N lifetimes are included using the `time_of_flight` option in MADGRAPH5.

The generated events are then interfaced to PYTHIA8 v2.15 [60] for hadronization and computation of the N decays. We use FASTJET 3.1.3 [61] for jet and trackless jet reconstruction. Lepton reconstruction and the identification of the displaced vertices is also done inside PYTHIA8. The masses and decay widths of the particles in the model are communicated to PYTHIA via the SLHA [62,63] section of the LHE header. Plots are generated with `matplotlib` [64].

The ATLAS analysis in Ref. [38] looks for high track-multiplicity displaced vertices at 13 TeV in events possessing displaced vertices and missing transverse momenta. We follow the detailed prescription using parametrized selection efficiencies as a function of displaced vertex radial distance, number of tracks and mass, that can be applied to vertices passing certain particle-level acceptance requirements using the truth Monte Carlo event record. These efficiencies can be found in Ref. [36], and are given for different regions in the detector, encapsulating also the effect of the material veto cut the analysis implements to remove background vertices.[1]

The analysis in Ref. [38] originally triggered on missing transverse momenta in the event that was bigger than 250 GeV. In this work, we propose to trigger on the prompt lepton coming from the W_R decay,[2] as in our model there is little or no missing transverse momenta. Apart from the trigger requirement, we fully recast the multitrack analysis in Ref. [38].

We require events to satisfy the following selections.

(1) Prompt electron: One electron[3] with $p_T > 25$ GeV.

(2) Trackless jet: One "trackless jet" with $p_T > 70$ GeV, or two trackless jets with $p_T > 25$ GeV. A trackless jet is defined as a jet for which the scalar sum of the p_T of all charged particles inside the jet does not exceed 5 GeV.[4]

In addition, each event must have at least one displaced vertex with the following.

(3) DV fiducial: Distance between the interaction point and the decay position > 4 mm. The decay position must also lie in the fiducial region $r_{DV} < 300$ mm and $|z_{DV}| < 300$ mm.

(4) DV N_{trk}: The number of selected decay products must be at least five, where selected decay products

are charged and stable, with $p_T > 1$ GeV and transverse impact parameter $|d_0| > 2$ mm.

(5) DV m_{DV}: The invariant mass of the truth vertex must be larger than 10 GeV, and is constructed assuming all charged decay products have the mass of the pion.

(6) DV efficiency: Parametrized selection efficiencies are implemented depending on the displaced vertex distance, number of tracks and mass, following the prescription in Ref. [36].

Based on these cuts, we first study the neutrino masses the analysis can be sensitive to. We simulate a grid of points with $m_N = [10$–$80]$ GeV and $m_{W_R} = [2$–$5]$ TeV. At each point we calculate the neutrino decay length, given by $c\tau_N \langle \beta\gamma \rangle$, where the average of the $\beta\gamma$ factor is taken after 10 000 events, and it is roughly $\mathcal{O}(100)$ for the scanned grid.

Figure 2 shows the dependence on the decay position with the W_R mass, for fixed values of the sterile neutrino mass. We note that for $m_N > 40$ GeV, decays are below 4 mm, and will therefore fail to be in the fiducial region required by the analysis. An optimal acceptance region lies between 10 GeV $< m_N < 40$ GeV and 2 TeV $< m_{W_R} < 5$ TeV.

We therefore choose a particular benchmark point with $m_N = 20$ GeV and $m_{W_R} = 4$ TeV, and proper neutrino decay distance $c\tau_N = 1.3$ mm. We show the effect of applying all analysis cuts on this benchmark in Table I.

We see very low efficiency, reaching 0.06% in Table I. The loss comes mainly from the last two cuts—$N_{trk} \geq 5$ and invariant vertex mass $m_{DV} > 10$ GeV—which are too restrictive for the given neutrino mass of $m_N = 20$ GeV, as softer decay products will lead to a smaller amount of tracks available to make up a vertex. This sensitivity loss was also noted in a model with a long-lived singlino

FIG. 2. Sterile neutrino decay distance as a function of W_R mass, for fixed values of the sterile neutrino mass. The upper right plot shows a zoomed region, where higher neutrino mass curves can be seen.

---

[1]The parametrized efficiencies provided by the ATLAS analysis were validated in Refs. [65,66].

[2]The ATLAS 8 TeV [37] version of this analysis considers a DV + lepton signature, where the lepton that fires the trigger is associated with the displaced vertex. Here we do not follow this approach, as the decay products of the displaced N are too collimated for the displaced lepton to satisfy isolation requirements. Alternatively, a "trackless jet trigger" [67]— where a jet matched with a muon is required—could be used to trigger on events, although it was shown that this trigger is inefficient for reconstructing displaced vertices within the tracker [68].

[3]Note that in our simplified model we consider mixing in the electron sector only, so the prompt lepton is an electron. In the case where muon mixing is present, a muon trigger can be used.

[4]This requirement is applied offline when processing data on disk, and is part of the first filtering in Ref. [38] that gives the data set where the *large-radius tracking* is applied to. Therefore, this trackless jet cut can only see prompt tracks, so a particle decaying inside the tracker can pass this selection.
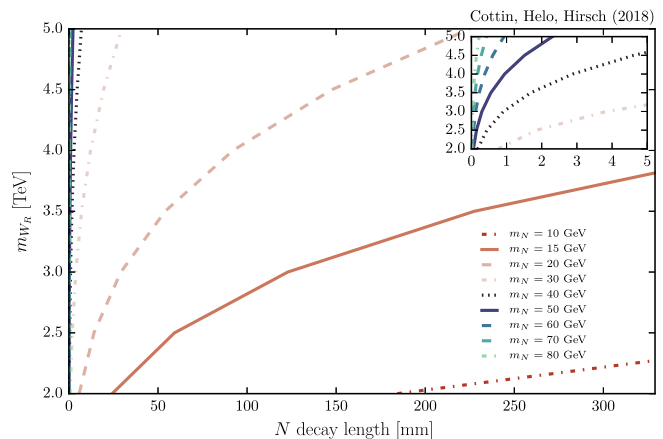
TABLE I. Numbers of simulated events N at $\sqrt{s} = 13$ TeV, relative and overall efficiencies for our left-right model with $m_N = 20$ GeV, $m_{W_R} = 4$ TeV and $c\tau_N = 1.3$ mm, for the ATLAS default cuts.

	N	Rel. ϵ [%]	Ov. ϵ [%]
All events	10 000	100	100
Prompt electron	8721	87.2	87.2
Trackless jet	8704	99.8	87.0
DV fiducial	7615	87.5	76.1
DV N_{trk}	528	6.9	5.3
DV m_{DV}	89	16.9	0.9
DV efficiency	6	6.7	0.06

decaying to a light ($\sim$20 GeV) pseudoscalar [69], and in a model with displaced Higgs decays to light ($\sim$10 GeV) hidden scalars [68].

We attempt to improve the sensitivity by loosening the N_{trk} and m_{DV} cuts, requiring $N_{\text{trk}} > 3$ and $m_{\text{DV}} \geq 5$ GeV.
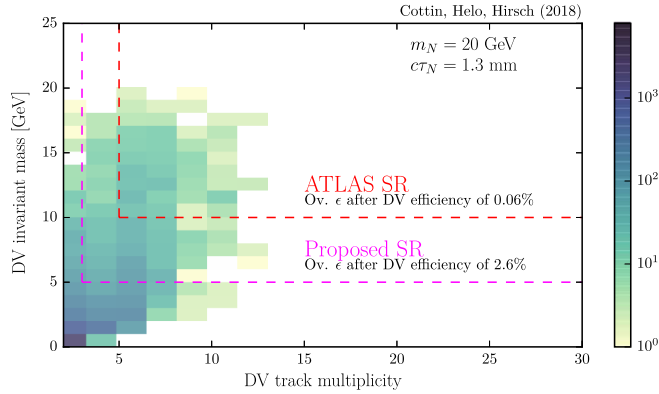

FIG. 3. Invariant mass of the displaced vertex against number of tracks for our left-right model with $m_N = 20$ GeV, $m_{W_R} = 4$ TeV and $c\tau_N = 1.3$ mm. Our proposed signal region is defined by the $N_{\text{trk}} > 3$ and $m_{\text{DV}} \geq 5$ GeV cuts.

We should note that, even though the backgrounds to the multitrack displaced vertex search come mostly from instrumental sources (including hadronic interactions in dense material regions and random crossing of tracks), lowering the invariant mass and track multiplicity cuts could in principle increase background rates. Nevertheless, we expect these to still be within negligible levels with the requirements of displaced activity (i.e. d_0 and trackless jet cut). In addition, there are still no background yields reported by ATLAS in this relaxed region, as it can be seen in Fig. 7 of Ref. [38]. Of course, a dedicated experimental background estimation study with these optimized cuts would be needed, which is beyond the capabilities of our detector simulations.

Figure 3 shows the invariant mass of the displaced vertex against the number of tracks for our benchmark. Prompt electron, Trackless jet and DV fiducial cuts are applied (cuts 1. to 3.). The last two cuts of DV N_{trk} and DV m_{DV} (cuts 4. and 5.) define the regions where signal is expected to be found (SR) and are shown as dashed boxes in the figure. The red box defines a SR with the default ATLAS cuts of $N_{\text{trk}} \geq 5$ and $m_{\text{DV}} > 10$ GeV. The purple box defines our proposed SR with $N_{\text{trk}} > 3$ and $m_{\text{DV}} \geq 5$ GeV. In each boxed region we show the final efficiency obtained after applying the experimental DV efficiency (cut 6.). We see an efficiency improvement of 2 orders of magnitude in our proposed SR.

With the proposed tuned cuts of $N_{\text{trk}} > 3$ and $m_{\text{DV}} \geq 5$ GeV we now discuss discovery prospects. Figure 4 shows the number of signal events in the mass plane $m_{W_R} - m_N$. Regions producing at least three signal events are shown, which is reasonable to set as a requirement for discovery in the absence of background. We see in the left plot of Fig. 4 that at 13 TeV and with 300 fb^{-1} the LHC is sensitive to masses up to $m_N \sim 20$ GeV, for $m_{W_R} \sim 3.5$ TeV. With a higher luminosity of 3000 fb^{-1} in the right plot, the 13 TeV LHC can reach sterile neutrino masses up to $\sim$30 GeV for similar W_R masses.
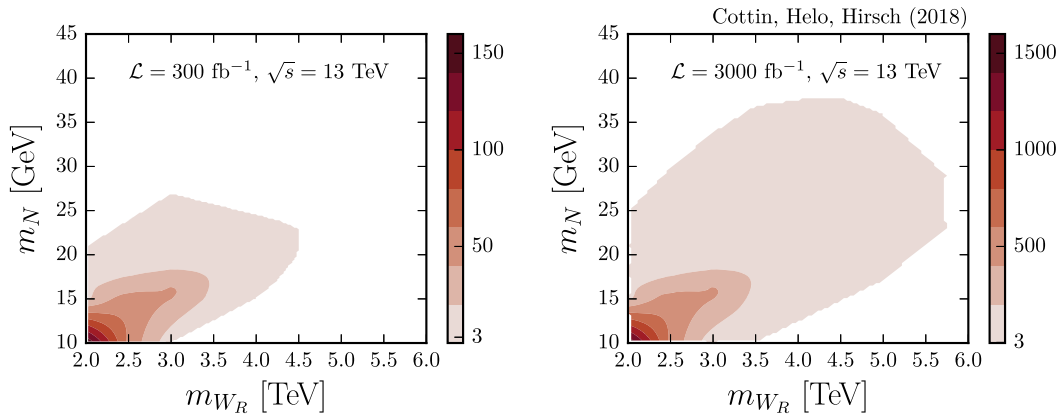

FIG. 4. Number of signal events for our left-right model at $\sqrt{s} = 13$ TeV, with our proposed search strategy, with $\mathcal{L} = 300$ fb^{-1} (left) and $\mathcal{L} = 3000$ fb^{-1} (right).

IV. SUMMARY AND CONCLUSIONS

We have studied the sensitivity of current multitrack displaced vertex searches at the LHC for probing long-lived, light sterile neutrinos. We based our study on a left-right symmetric model, and considered sterile neutrino masses $m_N \ll m_{W_R}$, and $m_N < m_W$.

We found that for 40 GeV $< m_N <$ 80 GeV, neutrino decay distances are below 4 mm, and will therefore fail to be in the analysis fiducial tracker region.

After considering a different trigger strategy on the prompt lepton in the event, we found very poor signal efficiency for events passing the standard DV cuts. This is due to the low mass of the sterile neutrino, as it is too soft to produce much tracks.

After loosening the DV invariant mass and number of tracks to a region where still zero background is reported [38], we found that with 3000 fb^{-1} of integrated luminosity at 13 TeV, this proposed "loose multitrack DV + prompt lepton" search should be sensitive to sterile neutrino masses up to ~30 GeV.

The identification of displaced vertices will continue to be an important signature of new physics, given that this signal is scarce in the SM. We encourage the experimental collaborations at the LHC to pursue these searches further, particularly in the study of lower cuts in the displaced vertex invariant mass, as m_N lower than 10 GeV may be probed.

[1] G. Aad *et al.* (ATLAS Collaboration), Phys. Lett. B **716**, 1 (2012).

[2] S. Chatrchyan *et al.* (CMS Collaboration), Phys. Lett. B **716**, 30 (2012).

[3] K. A. Olive *et al.* (Particle Data Group), Chin. Phys. C **38**, 090001 (2014).

[4] P. Minkowski, Phys. Lett. B **67**, 421 (1977).

[5] R. N. Mohapatra and G. Senjanovic, Phys. Rev. Lett. **44**, 912 (1980).

[6] J. Schechter and J. W. F. Valle, Phys. Rev. D **22**, 2227 (1980).

[7] K. N. Abazajian *et al.*, arXiv:1204.5379.

[8] Y. Cai, T. Han, T. Li, and R. Ruiz, arXiv:1711.02180.

[9] F. F. Deppisch, P. S. Bhupal Dev, and A. Pilaftsis, New J. Phys. **17**, 075019 (2015).

[10] A. Atre, T. Han, S. Pascoli, and B. Zhang, J. High Energy Phys. 05 (2009) 030.

[11] J. C. Pati and A. Salam, Phys. Rev. D **10**, 275 (1974); **11**, 703(E) (1975).

[12] R. N. Mohapatra and J. C. Pati, Phys. Rev. D **11**, 2558 (1975).

[13] W.-Y. Keung and G. Senjanovic, Phys. Rev. Lett. **50**, 1427 (1983).

[14] A. Datta, M. Guchait, and A. Pilaftsis, Phys. Rev. D **50**, 3195 (1994).

[15] O. Panella, M. Cannoni, C. Carimalo, and Y. N. Srivastava, Phys. Rev. D **65**, 035005 (2002).

[16] T. Han and B. Zhang, Phys. Rev. Lett. **97**, 171804 (2006).

[17] F. del Aguila, J. A. Aguilar-Saavedra, and R. Pittau, J. High Energy Phys. 10 (2007) 047.

[18] L. Basso, A. Belyaev, S. Moretti, and C. H. Shepherd-Themistocleous, Phys. Rev. D **80**, 055030 (2009).

[19] P. Fileviez Perez, T. Han, and T. Li, Phys. Rev. D **80**, 073015 (2009).

[20] J. N. Ng, A. de la Puente, and B. W.-P. Pan, J. High Energy Phys. 12 (2015) 172.

[21] P. Cox, C. Han, and T. T. Yanagida, J. High Energy Phys. 01 (2018) 037.

[22] A. Das, P. Konar, and A. Thalapillil, J. High Energy Phys. 02 (2018) 083.

[23] C. O. Dib, C. S. Kim, N. A. Neill, and X.-B. Yuan, Phys. Rev. D **97**, 035022 (2018).

[24] S. Antusch, E. Cazzato, and O. Fischer, Phys. Lett. B **774**, 114 (2017).

[25] E. Accomando, L. Delle Rose, S. Moretti, E. Olaiya, and C. H. Shepherd-Themistocleous, J. High Energy Phys. 02 (2018) 109.

[26] P. S. B. Dev, R. N. Mohapatra, and Y. Zhang, Nucl. Phys. **B923**, 179 (2017).

[27] S. Antusch, E. Cazzato, and O. Fischer, J. High Energy Phys. 12 (2016) 007.

[28] S. Antusch, E. Cazzato, and O. Fischer, Int. J. Mod. Phys. A **32**, 1750078 (2017).

[29] S. Dube, D. Gadkari, and A. M. Thalapillil, Phys. Rev. D **96**, 055031 (2017).

[30] M. Mitra, R. Ruiz, D. J. Scott, and M. Spannowsky, Phys. Rev. D **94**, 095016 (2016).

[31] E. Accomando, L. Delle Rose, S. Moretti, E. Olaiya, and C. H. Shepherd-Themistocleous, J. High Energy Phys. 04 (2017) 081.

[32] E. Izaguirre and B. Shuve, Phys. Rev. D **91,** 093010 (2015).

[33] A. M. Gago, P. Hernández, J. Jones-Pérez, M. Losada, and A. Moreno Briceño, Eur. Phys. J. C **75,** 470 (2015).

[34] C. Dib and C. S. Kim, Phys. Rev. D **89,** 077301 (2014).

[35] J. C. Helo, M. Hirsch, and S. Kovalenko, Phys. Rev. D **89,** 073005 (2014); **93,** 099902(E) (2016).

[36] https://atlas.web.cern.ch/Atlas/GROUPS/PHYSICS/PAPERS/SUSY-2016-08/hepdata_info.pdf.

[37] G. Aad *et al.* (ATLAS Collaboration), Phys. Rev. D **92,** 072004 (2015).

[38] M. Aaboud *et al.* (ATLAS Collaboration), arXiv:1710.04901.

[39] R. N. Mohapatra and G. Senjanovic, Phys. Rev. D **23,** 165 (1981).

[40] O. Castillo-Felisola, C. O. Dib, J. C. Helo, S. G. Kovalenko, and S. E. Ortiz, Phys. Rev. D **92,** 013001 (2015).

[41] A. Maiezza, M. Nemevšek, and F. Nesti, Phys. Rev. Lett. **115,** 081802 (2015).

[42] G. Aad *et al.* (ATLAS Collaboration), J. High Energy Phys. 07 (2015) 162.

[43] V. Khachatryan *et al.* (CMS Collaboration), Eur. Phys. J. C **74,** 3149 (2014).

[44] CMS Collaboration, Search for a heavy right-handed W boson and a heavy neutrino in events with two same-flavor leptons and two jets at $\sqrt{(s)} = 13$ TeV, Tech. Report No. CMS-PAS-EXO-17-011, 2017).

[45] G. Aad *et al.* (ATLAS Collaboration), Phys. Lett. B **754,** 302 (2016).

[46] V. Khachatryan *et al.* (CMS Collaboration), Phys. Rev. Lett. **116,** 071801 (2016).

[47] M. Aaboud *et al.* (ATLAS Collaboration), Phys. Rev. D **96,** 052004 (2017).

[48] S. Chatrchyan *et al.* (CMS Collaboration), Phys. Lett. B **701,** 160 (2011).

[49] M. Aaboud *et al.* (ATLAS Collaboration), arXiv:1706.04786.

[50] M. Nemevsek, F. Nesti, G. Senjanovic, and Y. Zhang, Phys. Rev. D **83,** 115014 (2011).

[51] M. Nemevšek, F. Nesti, and G. Popara, arXiv:1801.05813.

[52] V. Khachatryan *et al.* (CMS Collaboration), Phys. Rev. D **91,** 012007 (2015).

[53] C. Degrande, C. Duhr, B. Fuks, D. Grellscheid, O. Mattelaer, and T. Reiter, Comput. Phys. Commun. **183,** 1201 (2012).

[54] F. Staub, Comput. Phys. Commun. **185,** 1773 (2014).

[55] W. Porod and F. Staub, Comput. Phys. Commun. **183,** 2458 (2012).

[56] W. Porod, Comput. Phys. Commun. **153,** 275 (2003).

[57] C. Bonilla, M. E. Krauss, T. Opferkuch, and W. Porod, J. High Energy Phys. 03 (2017) 027.

[58] J. Alwall, R. Frederix, S. Frixione, V. Hirschi, F. Maltoni, O. Mattelaer, H. S. Shao, T. Stelzer, P. Torrielli, and M. Zaro, J. High Energy Phys. 07 (2014) 079.

[59] J. Alwall *et al.*, Comput. Phys. Commun. **176,** 300 (2007).

[60] T. Sjöstrand, S. Ask, J. R. Christiansen, R. Corke, N. Desai, P. Ilten, S. Mrenna, S. Prestel, C. O. Rasmussen, and P. Z. Skands, Comput. Phys. Commun. **191,** 159 (2015).

[61] M. Cacciari, G. P. Salam, and G. Soyez, Eur. Phys. J. C **72,** 1896 (2012).

[62] P. Z. Skands *et al.*, J. High Energy Phys. 07 (2004) 036.

[63] B. C. Allanach *et al.*, Comput. Phys. Commun. **180,** 8 (2009).

[64] J. D. Hunter, Computing In Science & Engineering **9,** 90 (2007).

[65] LHC-LLP community white paper (to be published).

[66] Les Houches Working Group report (to be published).

[67] G. Aad *et al.* (ATLAS Collaboration), J. Inst. **8,** P07015 (2013).

[68] C. Csaki, E. Kuflik, S. Lombardo, and O. Slone, Phys. Rev. D **92,** 073008 (2015).

[69] B. C. Allanach, M. Badziak, G. Cottin, N. Desai, C. Hugonie, and R. Ziegler, Eur. Phys. J. C **76,** 482 (2016).

Correction: The previously published Figure 4 contained an error and has been replaced.